

INTERFERENCE ALIGNMENT IN UMTS LONG TERM EVOLUTION

Jörg Reitterer and Markus Rupp

Institute of Telecommunications, Vienna University of Technology
 Gußhausstraße 25/389, A-1040 Vienna, Austria
 Email: {jreitter, mrupp}@nt.tuwien.ac.at

ABSTRACT

In this paper the performance of interference alignment is evaluated for the downlink of 3GPP UMTS LTE via the *Vienna LTE Link Level simulator*. Interference alignment is compared to closed-loop spatial multiplexing, a non-cooperative communication scheme. In order to reduce the computational complexity of solving the interference alignment problem for each subcarrier separately, the same precoding and interference suppression matrices are used for disjoint subsets of subcarriers. The performance impairment in terms of average throughput reduction of this approach is analyzed numerically. Furthermore, the performance of interference alignment is investigated for realistic fast-fading channels employing outdated precoding and interference suppression matrices.

1. INTRODUCTION

Interference alignment (IA) is a cooperative transmission strategy for the interference channel that results in a linearly scaling sum-rate with the number of users in the system in the high SNR regime [1]. IA is based only on linear precoding at the transmitters and zero-forcing at the receivers but requires extensive channel knowledge in order to sufficiently suppress the interference at all receivers simultaneously [2]. The key idea of IA is to use precoding matrices at all transmitters such that the interference aligns at each receiver and spans only a subspace of the receive space, thus providing interference free subspaces for the desired signals. In some simple scenarios there exist closed-form solutions of the IA problem [1]. For scenarios with arbitrary number of users, transmit and receive antennas as well as number of spatial streams, iterative algorithms were introduced in [3–5]. In [6] IA feasibility conditions were derived for certain scenarios, while they are still unknown for arbitrary scenarios.

The goal of this paper is to evaluate the performance of IA in the downlink of 3GPP UMTS Long Term Evolution (LTE) [7] by employing the *Vienna LTE Link Level simulator* [8–10]. Due to the high computational complexity, only simple scenarios incorporating three transmitter-receiver pairs are investigated, i.e. three eNodeBs with one user connected to each eNodeB. For these scenarios there exists a closed-form solution of the IA problem. Since LTE is based on Orthogonal Frequency Division Multiple-Access (OFDMA), which introduces a frequency orthogonality of the separate subcarriers, IA can be applied independently inside each OFDM subband [2]. On the other hand, the computational complexity of solving the IA problem for each subcarrier separately can be prohibitively large for a large number of subcarriers. We therefore investigate the performance impairment when applying a coarser IA granularity, i.e. using the same precoding and interference suppression matrices for

disjoint subsets of subcarriers. Furthermore, we investigate the performance of IA in fast fading channels with different granularity in the time domain, i.e. employing outdated precoding matrices and interference suppression matrices.

This article is organized as follows: The system model and the application of IA to LTE are introduced in Section 2. Section 3 describes the concept of IA granularity in the time and frequency domain, while Section 4 presents simulation results obtained by the *Vienna LTE Link Level simulator*. Section 5 concludes the paper.

2. LTE INTERFERENCE ALIGNMENT SYSTEM MODEL

Figure 1 depicts IA for $K = 3$ transmitter-receiver pairs with $d_1 = d_2 = d_3 = 2$ spatial streams. In this example each transmitter has $N_T = 4$ transmit antennas and each receiver has $N_R = 4$ receive antennas. The index $n \in [1, N]$ indicates the subcarrier index.

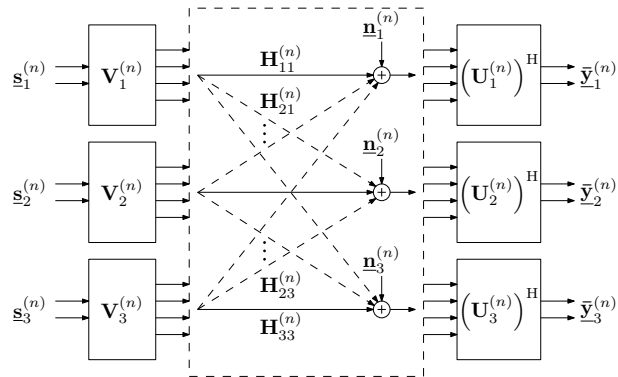


Figure 1: IA in an OFDM system incorporating $K = 3$ transmitter-receiver pairs.

The received signal of user i at subcarrier n after interference suppression is given by [2]

$$\begin{aligned} \bar{\mathbf{y}}_i^{(n)} &= \underbrace{\left(\mathbf{U}_i^{(n)}\right)^H \mathbf{H}_{ii}^{(n)} \mathbf{V}_i^{(n)} \mathbf{s}_i^{(n)}}_{\text{Desired signal of user } i} \\ &+ \underbrace{\sum_{j \neq i} \left(\mathbf{U}_i^{(n)}\right)^H \mathbf{H}_{ij}^{(n)} \mathbf{V}_j^{(n)} \mathbf{s}_j^{(n)}}_{\text{Interference from users } j \neq i} + \underbrace{\left(\mathbf{U}_i^{(n)}\right)^H \mathbf{n}_i^{(n)}}_{\text{Effective noise}} \quad (1) \end{aligned}$$

$$= \left(\mathbf{U}_i^{(n)}\right)^H \mathbf{H}_{ii}^{(n)} \mathbf{V}_i^{(n)} \mathbf{s}_i^{(n)} + \left(\mathbf{U}_i^{(n)}\right)^H \mathbf{n}_i^{(n)} \quad (2)$$

$$= \bar{\mathbf{H}}_{ii}^{(n)} \mathbf{s}_i^{(n)} + \bar{\mathbf{n}}_i^{(n)}, \quad \forall n = 1, \dots, N. \quad (3)$$

Here, $\underline{s}_i^{(n)}$ is the d_i dimensional signal vector of eNodeB i and subcarrier n and $\underline{s}_j^{(n)}$ is the d_j dimensional signal vector of the interfering eNodeB j , respectively. Furthermore, $\underline{n}_i^{(n)}$ is the $N_{R,i}$ dimensional additive noise vector¹ at receiver i and $\mathbf{V}_i^{(n)}$ and $(\mathbf{U}_i^{(n)})^H$ are the precoding matrices of transmitter i and interference suppression matrices of receiver i , respectively. IA of subcarrier n is achieved if and only if the equations

$$(\mathbf{U}_i^{(n)})^H \mathbf{H}_{ij}^{(n)} \mathbf{V}_j^{(n)} = 0, \quad \forall j \neq i \quad (4)$$

$$\text{rank} \left[(\mathbf{U}_i^{(n)})^H \mathbf{H}_{ii}^{(n)} \mathbf{V}_j^{(n)} \right] = d_i \quad (5)$$

are fulfilled [1].

Figure 2 shows the schematic of the LTE transmitter, applying separate precoding matrices for each of the N subcarriers not null. Each of the d_i spatial streams is converted to N parallel streams, where N is the total number of subcarriers not null. Each subcarrier $n = 1, \dots, N$ is then precoded individually employing the IA precoding matrix $\mathbf{V}_i^{(n)}$. The rest of the $N_{T,i}$ OFDM modulation chains consist of zero padding (ZP), inverse fast Fourier transformation (IFFT), parallel-to-serial conversion, and insertion of a cyclic prefix (CP).

Figure 3 shows an LTE IA receiver with a total of N different interference suppression matrices $(\mathbf{U}_i^{(n)})^H$, one for each subcarrier. Here, the $N_{R,i}$ OFDM demodulation chains consist of CP removal, serial-to-parallel conversion, fast Fourier transformation (FFT), and ZP removal.

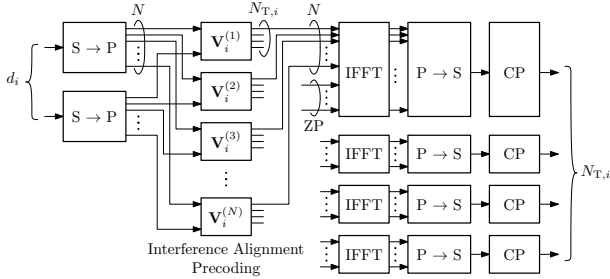


Figure 2: LTE transmitter with separate precoding matrices for each subcarrier.

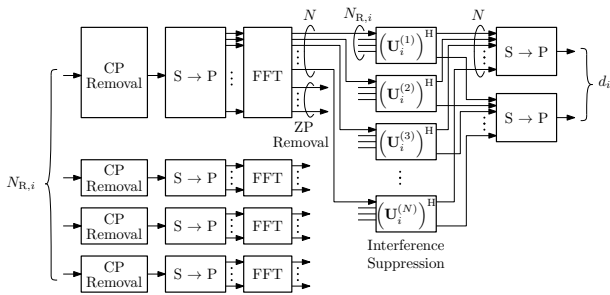


Figure 3: LTE receiver with separate interference suppression matrices for each subcarrier.

3. GRANULARITY OF INTERFERENCE ALIGNMENT

3.1 Spectral Interference Alignment Granularity

As already mentioned, the computational complexity of solving the IA problem for each subcarrier separately can be prohibitively large for a large number of subcarriers. In order to reduce complexity, the total set of N subcarriers can be split into M disjoint subsets \mathcal{N}_k with $\bigcup_{k=1}^M \mathcal{N}_k = \{1, 2, \dots, N\}$ and IA is calculated within these subsets. Here, only subsets of equal length ξ_f will be investigated for the sake of simplicity². Figure 4 shows the separation of the N subcarriers into the $M = N/\xi_f$ disjoint subsets with corresponding precoding matrices $\tilde{\mathbf{V}}_i^{(k)}$.

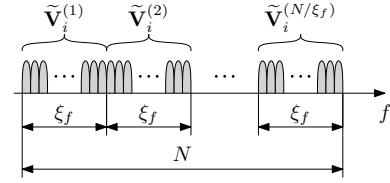


Figure 4: Definition of the spectral IA granularity ξ_f .

For the calculation of the N/ξ_f different precoding matrices $\tilde{\mathbf{V}}_i^{(k)}$ and the corresponding interference suppression matrices $(\tilde{\mathbf{U}}_i^{(k)})^H$ the channel matrices are averaged over spectral intervals of ξ_f subcarriers, i.e.

$$\tilde{\mathbf{H}}_{ij}^{(k)} = \frac{1}{\xi_f} \sum_{n=(k-1)\xi_f+1}^{k\xi_f} \mathbf{H}_{ij}^{(n)}, \quad k = 1, \dots, N/\xi_f. \quad (6)$$

For $K = 3$ users, $N_{T,i} = N_{R,i} = N_{T,R}$, $i = 1, 2, 3$ and $d_1 = d_2 = d_3 = d$ there exists a closed-form solution of the IA problem [1] if the feasibility conditions from [6] are satisfied. The precoding matrices have to fulfill

$$\text{span} \left(\tilde{\mathbf{V}}_1^{(k)} \right) = \text{span} \left(\tilde{\mathbf{E}}^{(k)} \tilde{\mathbf{V}}_1^{(k)} \right), \quad (7)$$

$$\tilde{\mathbf{V}}_2^{(k)} = \left(\tilde{\mathbf{H}}_{32}^{(k)} \right)^{-1} \tilde{\mathbf{H}}_{31}^{(k)} \tilde{\mathbf{V}}_1^{(k)}, \quad (8)$$

$$\tilde{\mathbf{V}}_3^{(k)} = \left(\tilde{\mathbf{H}}_{23}^{(k)} \right)^{-1} \tilde{\mathbf{H}}_{21}^{(k)} \tilde{\mathbf{V}}_1^{(k)}, \quad (9)$$

where

$$\tilde{\mathbf{E}}^{(k)} = \left(\tilde{\mathbf{H}}_{31}^{(k)} \right)^{-1} \tilde{\mathbf{H}}_{32}^{(k)} \left(\tilde{\mathbf{H}}_{12}^{(k)} \right)^{-1} \tilde{\mathbf{H}}_{13}^{(k)} \left(\tilde{\mathbf{H}}_{23}^{(k)} \right)^{-1} \tilde{\mathbf{H}}_{21}^{(k)}. \quad (10)$$

The matrix $\tilde{\mathbf{E}}^{(k)}$ has $N_{T,R}$ eigenvectors $\underline{e}_1, \underline{e}_2, \dots, \underline{e}_{N_{T,R}}$. The precoding matrix of transmitter 1 consists of any d of these eigenvectors, i.e. $\tilde{\mathbf{V}}_1^{(k)} = [\underline{e}_1, \underline{e}_2, \dots, \underline{e}_d]$. The other two precoding matrices $\tilde{\mathbf{V}}_2^{(k)}$ and $\tilde{\mathbf{V}}_3^{(k)}$ can be calculated by Equations (8)–(9). The interference suppression matrices $(\tilde{\mathbf{U}}_i^{(k)})^H$ are obtained by calculating the left null space of the received

¹Here, the noise is modeled as additive white Gaussian noise (AWGN).

²The generalization of this concept for subsets of arbitrary length is straightforward.

interference, i.e.

$$\tilde{\mathbf{U}}_1^{(k)} = \text{null} \left[\left(\tilde{\mathbf{H}}_{12}^{(k)} \tilde{\mathbf{V}}_2^{(k)} \right)^H \right] = \text{null} \left[\left(\tilde{\mathbf{H}}_{13}^{(k)} \tilde{\mathbf{V}}_3^{(k)} \right)^H \right], \quad (11)$$

$$\tilde{\mathbf{U}}_2^{(k)} = \text{null} \left[\left(\tilde{\mathbf{H}}_{21}^{(k)} \tilde{\mathbf{V}}_1^{(k)} \right)^H \right] = \text{null} \left[\left(\tilde{\mathbf{H}}_{23}^{(k)} \tilde{\mathbf{V}}_3^{(k)} \right)^H \right], \quad (12)$$

$$\tilde{\mathbf{U}}_3^{(k)} = \text{null} \left[\left(\tilde{\mathbf{H}}_{31}^{(k)} \tilde{\mathbf{V}}_1^{(k)} \right)^H \right] = \text{null} \left[\left(\tilde{\mathbf{H}}_{32}^{(k)} \tilde{\mathbf{V}}_2^{(k)} \right)^H \right]. \quad (13)$$

Since here in general

$$\tilde{\mathbf{V}}_i^{(k)} \neq \mathbf{V}_i^{(n)}, n \in [(k-1)\xi_f + 1, k\xi_f], \quad (14)$$

$$\tilde{\mathbf{U}}_i^{(k)} \neq \mathbf{U}_i^{(n)}, n \in [(k-1)\xi_f + 1, k\xi_f], \quad (15)$$

a perfect alignment of the interference at the receivers will not be possible and there will be some residual interference in the desired receive signal subspaces. In Section 4 we will investigate numerically how this trade-off between residual interference and reduction in computational complexity affects the average throughput in a 3GPP UMTS LTE system.

3.2 Temporal Interference Alignment Granularity

Similar to the spectral IA granularity ξ_f in the frequency domain we can define a temporal IA granularity ξ_t in the time domain. Here, ξ_t denotes the number of OFDM symbols for which the same precoding and interference suppression matrices are used, e.g. $\xi_t = 14$ means that same set of N precoding matrices remains during one subframe of duration $T_{\text{sub}} = 1$ ms. Due to both, the high computational complexity and the large feedback overhead, in a realistic system $\xi_t > 1$ which results in residual interference in the receive signal spaces and, hence, a throughput reduction in a fast-fading channel. The feedback overhead itself is not taken into account in this work.

4. SIMULATION RESULTS

This section presents simulation results obtained by the standard compliant *Vienna LTE Link Level simulator* [8]. The simulator package for link level simulations as well as the counterpart for system level simulations can freely be downloaded under an academic license agreement, supporting reproducible results. Currently, more than 6000 users of this environment exist worldwide.

In all simulations there is one user connected to each of the $K = 3$ eNodeBs and all eNodeBs share the same time-frequency resources simultaneously. The most important parameters of the simulations are summarized in Table 1.

Table 1: Simulation parameters.

Parameter	Value
System bandwidth	1.4 MHz
Number of subcarriers N	72
Number of eNodeBs K	3
Channel Models	Flat Rayleigh
	ITU-T PedA [11]
	ITU-T VehA [11]
Antenna configuration	2 transmit, 2 receive (2×2)
Receiver	Zero Forcing ZF
IA algorithm	Closed-form [1]

Figures 5(a) and 5(b) compare the average throughput of closed-loop spatial multiplexing (CLSM) and IA, respectively, as a function of both signal to noise ratio (SNR) and signal to interference ratio (SIR)³. CLSM employs the maximum number of spatial streams, i.e. $d_1 = d_2 = d_3 = 2$, while IA uses only $d_1 = d_2 = d_3 = 1$ spatial streams. This is due to the general fact, that IA allows virtually interference-free communications at the cost of each user exploiting only half of its available degrees of freedom [2]. Therefore, at high SIR and SNR the average throughput of CLSM is twice the average throughput of IA. As the SIR decreases, the average throughput in the CLSM case also decreases and at SIR = 0 dB there is no communication at all possible due to the strong interference. On the other hand, under IA the average throughput is—assuming perfect channel knowledge—*independent* of the SIR. Due to the trade-off between sacrificing half of the available degrees of freedom on the one hand and the ability to cancel the interference on the other, IA is only beneficial in terms of average throughput if the SIR is below a certain threshold, which depends on the CQI⁴ value. In a more realistic scenario, where global perfect channel knowledge is not available, the average throughput of course also decreases with decreasing SIR value in the IA case because of the nonzero residual interference in the receive signal subspace.

Figure 6 shows the average throughput as a function of the spectral IA granularity ξ_f for different SNR and CQI values. Here, we assume block-fading channel models with constant channels during one subframe duration of $T_{\text{sub}} = 1$ ms and channel realizations independent between subframes. All the receivers and transmitters are assumed to have perfect channel knowledge without any feedback or IA computation delay, meaning that the transmitters and receivers know the MIMO channel matrices $\mathbf{H}_{ij}^{(n)}$ *before* the actual transmission. The smaller the frequency selectivity of the channel, the coarser the spectral IA granularity can be for a specific throughput constraint. It is evident that the throughput does not depend on the spectral IA granularity for a flat Rayleigh channel, since here the channel matrices are the same for all subcarriers. Figure 6 also shows that at larger SNR and CQI the spectral IA granularity has to be finer, e.g. solving the IA problem on resource block level, i.e. $\xi_f = 12$, results in approximately 0% throughput for a VehA channel at SNR = 30 dB with CQI = 15 while at SNR = 15 dB with CQI = 9 the throughput is approximately 75% of the maximum value.

Figure 7 shows the average throughput as a function of the spectral IA granularity for different SIR values. The larger the SIR, the larger we can choose ξ_f for a given throughput constraint. A dynamical adaptation of the parameter ξ_f can significantly decrease computational complexity while keeping the throughput above a certain threshold.

In Figure 8 the average throughput is depicted as a function of the relative channel measurement error σ_H^2/σ_E^2 which stems from a noisy channel state information (CSI) $\tilde{\mathbf{H}} \neq \mathbf{H}$ [2]. Let $\mathbf{E} = \tilde{\mathbf{H}} - \mathbf{H}$ denote the channel measurement error,

³In order to analyze the effects of noise and interference on the throughput separately, SNR and SIR are used instead of signal to noise *and* interference ratio (SINR).

⁴The channel quality indicator (CQI) is employed to signal the supported adaptive modulation and coding scheme to the transmitter in order to achieve a target block error ratio, given the current channel conditions.

which is modeled as a complex Gaussian circularly symmetric random matrix with i.i.d. elements of variance σ_E^2 . Here, we employ flat Rayleigh channels with complex Gaussian i.i.d. unit variance elements of the channel matrices \mathbf{H}_{ij} , i.e. $\sigma_H^2 = 1$.

Figure 9 shows the average throughput as a function of the user velocity v for different values of the *temporal* IA granularity ξ_t . Here, we assume a ITU-T VehA fast-fading channel model with different channel realizations for each OFDM symbol. The *spectral* IA granularity is $\xi_f = 1$. Figure 9 shows that with a temporal alignment granularity of $\xi_t = 14$, i.e. the same set of N precoding matrices remains during one subframe, the average throughput decreases to 50% at a user velocity of just $v = 25$ km/h. Employing a temporal IA granularity of $\xi_t = 7$, the average throughput decreases to approximately 75%.

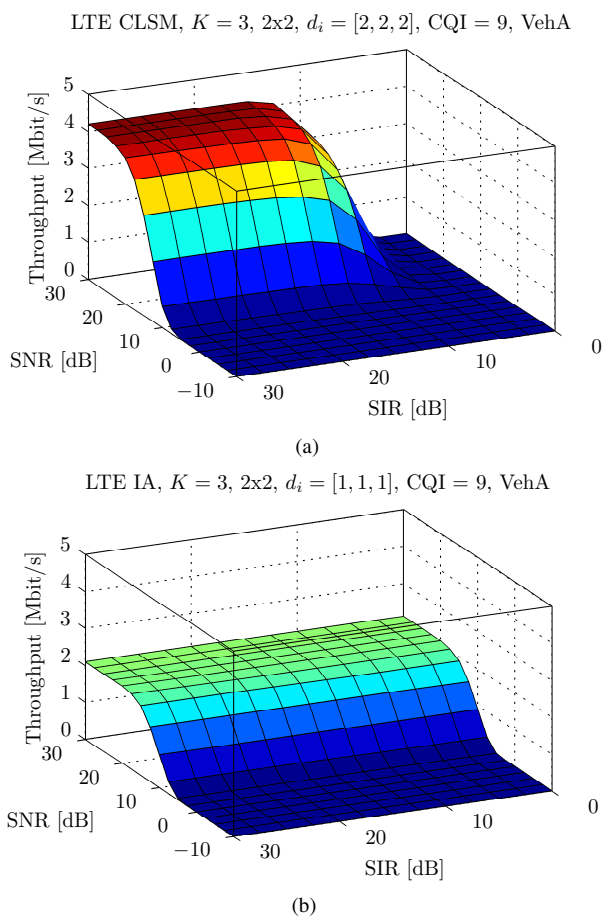


Figure 5: Average throughput vs. SNR and SIR for (a) CLSM and (b) IA.

5. CONCLUSION

In this paper interference alignment is evaluated in the context of 3GPP UMTS LTE via the *Vienna LTE Link Level simulator*. It is shown that IA only outperforms non-cooperative communication schemes like CLSM if the SIR is below a certain threshold. Depending on the degree of frequency selectivity of the channel the alignment can be computed for different spectral granularity, i.e. for disjoint sets of subcarriers of different size, in order to reduce the computational complexity. The performance impairment in terms of average throughput of employing outdated precoding and in-

terference suppression matrices is also shown as a function of the user velocity. Even at moderate user velocities the precoding and interference suppression matrices have to be updated in intervals shorter than one subframe in order to maintain a high average throughput.

ACKNOWLEDGMENT

This work has been funded by the Christian Doppler Laboratory for Wireless Technologies for Sustainable Mobility, KATHREIN-Werke KG, and A1 Telekom Austria AG. The financial support by the Federal Ministry of Economy, Family and Youth and the National Foundation for Research, Technology and Development is gratefully acknowledged.

REFERENCES

- [1] V. Cadambe and S. Jafar, "Interference alignment and degrees of freedom of the K -user interference channel," *Information Theory, IEEE Transactions on*, vol. 54, no. 8, pp. 3425–3441, 2008.
- [2] R. Tresh and M. Guillaud, "Cellular interference alignment with imperfect channel knowledge," in *Communications Workshops, 2009. ICC Workshops 2009. IEEE International Conference on*, pp. 1–5, 2009.
- [3] K. Gomadam, V. Cadambe, and S. Jafar, "Approaching the capacity of wireless networks through distributed interference alignment," in *Global Telecommunications Conference, 2008. IEEE GLOBECOM 2008. IEEE*, pp. 1–6, 2008.
- [4] S. Peters and R. Heath, "Interference alignment via alternating minimization," in *Acoustics, Speech and Signal Processing, 2009. ICASSP 2009. IEEE International Conference on*, pp. 2445–2448, 2009.
- [5] D. Schmidt, C. Shi, R. Berry, M. Honig, and W. Utschick, "Minimum mean squared error interference alignment," in *Signals, Systems and Computers, 2009 Conference Record of the Forty-Third Asilomar Conference on*, pp. 1106–1110, 2009.
- [6] C. Yetis, T. Gou, S. Jafar, and A. Kayran, "On feasibility of interference alignment in mimo interference networks," *IEEE Transactions on Signal Processing*, vol. 58, no. 9, pp. 4771–4782, 2010.
- [7] 3GPP, "Technical specification group radio access network; (E-UTRA) and (E-UTRAN); overall description; stage 2," 2008.
- [8] C. Mehlführer, M. Wrulich, J. C. Ikuno, D. Bosanska, and M. Rupp, "Simulating the long term evolution physical layer," in *Proc. of the 17th European Signal Processing Conference (EUSIPCO 2009)*, Aug. 2009.
- [9] C. Mehlführer, J. C. Ikuno, M. Simko, S. Schwarz, M. Wrulich, and M. Rupp, "The Vienna LTE simulators—enabling reproducibility in wireless communications research," *under review in Journal of Advances in Signal Processing special issue on Reproducibility in DSP*, 2011.
- [10] [Online]. Available <http://www.nt.tuwien.ac.at/ltesimulator/>.
- [11] ITU, "Recommendation ITU-R M.1225: Guidelines for evaluation of radio transmission technologies for IMT-2000," 1997.

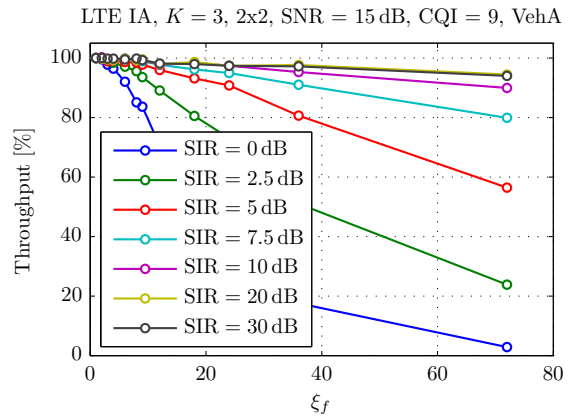
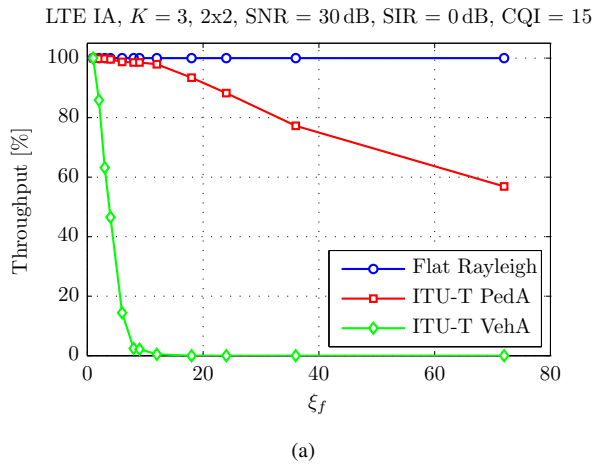


Figure 7: Average throughput as a function of the spectral IA granularity ξ_f for SIR values.

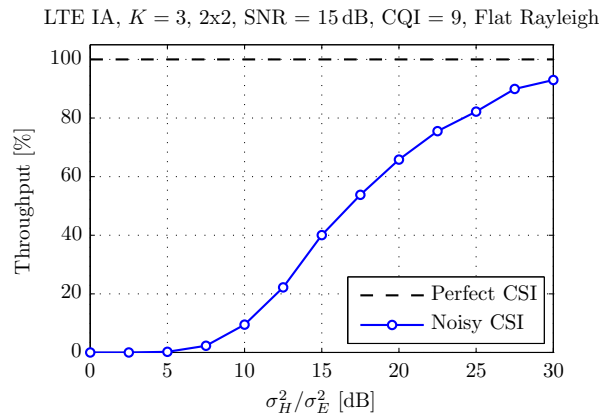
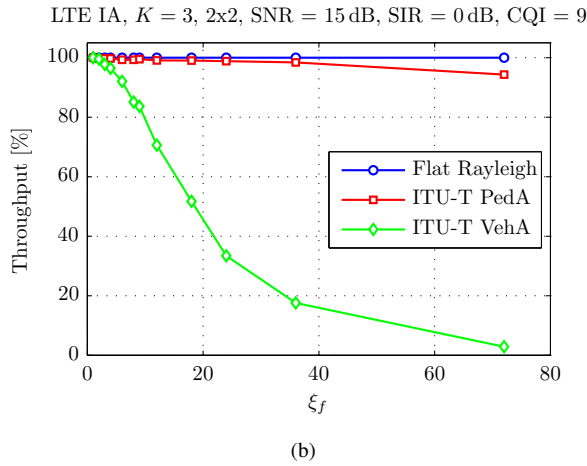


Figure 8: Average throughput as a function of the relative channel measurement error.

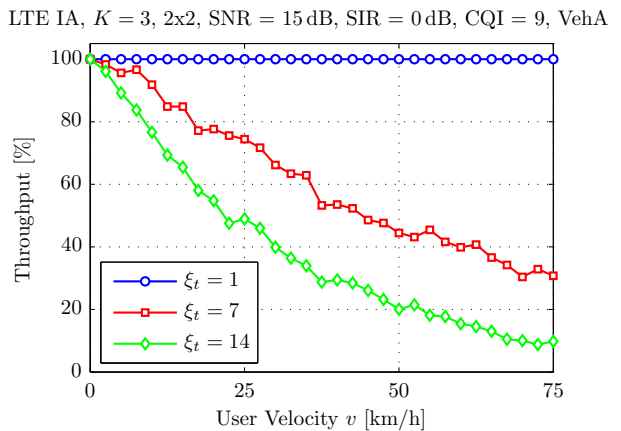
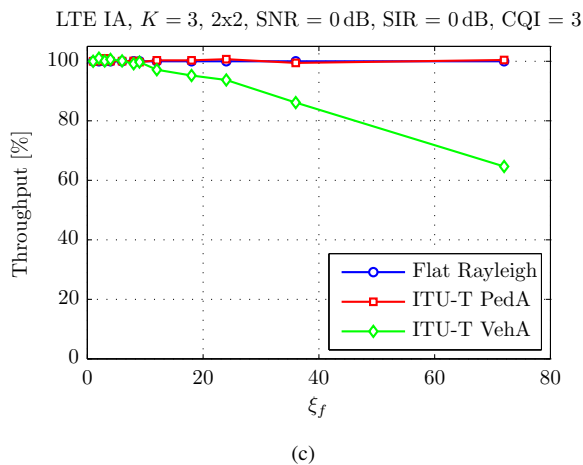


Figure 9: Average throughput as a function of the user velocity v in an ITU-T VehA channel for different values of the temporal IA granularity ξ_t .

Figure 6: Average throughput as a function of the spectral IA granularity ξ_f for different CQI and SNR values and various channel types.